

Studies on the lithosphere and the water transport by using the Japan Sea submarine cable (JASC): 1. Theoretical considerations

L. L. Vanyan¹, H. Utada², H. Shimizu², Y. Tanaka³, N. A. Palshin¹, V. Stepanov¹,
V. Kouznetsov¹, R. D. Medzhitov⁴, and A. Nozdrina¹

¹*Shirshov Institute of Oceanology, Moscow, Russia*

²*Earthquake Research Institute, University of Tokyo, Tokyo 113, Japan*

³*Faculty of Science, Kyoto University, Beppu 874, Japan*

⁴*Pacific Oceanographic Institute, Vladivostok, Russia*

(Received June 19, 1997; Revised November 21, 1997; Accepted November 25, 1997)

The Japan Sea Cable (JASC) was retired from telecommunications services and its ownership transferred to the scientific community in February, 1996. For the first stage of its scientific reuse program, a Japan-Russia joint project has been initiated to monitor electrical potential differences across the Japan Sea to study the electrical conductivity distribution in the Earth and the water transport across the cable.

This paper describes preliminary investigations by forward modelling study to explore possible results from the voltage observation, before analyzing real data. On the resistivity structure, modelling has suggested that voltage data is most sensitive to the conductance of resistive lithosphere, especially at longer periods. Water transport modelling has shown that the heterogeneity of sub-bottom resistivity does not greatly influence the cable voltage, and that water transport of 5–6 Sv in the Japan Sea can generate voltage differences of 70–80 mV across the JASC. A preliminary observation was found to be roughly consistent with this estimation.

1. Introduction

Coaxial transoceanic cables were installed during the 60's and 70's for international telecommunications purposes. Due to increasing demand for high-speed data transfer, they are now being retired from telecommunications services, replaced by modern fiber-optic systems. However these old systems are still very useful for scientific research in oceanic areas, which are not well covered by networks of various geophysical and oceanographic observations. Several efforts have recently been made to reuse such cable systems for scientific purposes (e.g., Kasahara *et al.*, 1995).

One of the simplest and most useful ways for scientific reuse of such cables is to measure natural electric potential variations over hundreds to thousands of kilometers (e.g., Lanzerotti *et al.*, 1993). Using potential variations over a large spacing, studies have been made on spatial characteristics of electric field variations induced by ionospheric and magnetospheric fields (Fujii *et al.*, 1995), on electrical conductivity distribution deep in the Earth (Lizarralde *et al.*, 1995), and on sea water transport that induces electromotive forces (Larsen, 1992). The Japan Sea Cable (JASC) connecting Nakhodka (Russia) and Naoetsu (Japan) was installed in 1969 by three owners: Kokusai Denshin Denwa, the Great Northern Telegraph Company and ROSTELECOM. In 1995 a new fiber-optic telephone cable was installed and, due to the courtesy of the owners, the JASC was given to Japanese and Russian scientists for joint experiments. Earthquake Research Institute of the University of Tokyo, Shirshov Institute of Oceanology and Pacific Oceanographic Institute (both

Russian Academy of Sciences) arranged a consortium for scientific reuse of the JASC. At the first stage of the joint project the cable voltage will be measured and analyzed. A possible outcome of the measurements is considered below.

The voltage measured by means of a submarine cable has two main sources: electric field induced by variations of the geomagnetic field of magnetosphere-ionosphere origin and motionally induced electric field. Thus, cable voltage measurements could be used to study the conductivity structure beneath the Sea of Japan and also to investigate the variability of the water velocity field. According to Faraday's law the electric field of the first source attenuates with frequency and for low frequencies (periods greater than 3–4 days) the motionally induced electric field usually dominates (Palshin, 1996; Flosadottir *et al.*, 1997). The theoretical investigation of motionally induced electric fields (Sanford, 1971; Chave and Luther, 1990) formed among other things the basis for the successful interpretation of submarine cable measurements in terms of water transport.

Magnetotelluric (MT) responses derived from the submarine cable measurements are significantly distorted by the coast effect, especially when cable spacing is relatively small. Since the distortion is mainly galvanic (so called "static shift") it would appear reasonable to combine cable MT response with some reference (not shifted) MT or magnetovariational (MV) response (e.g., Lizarralde *et al.*, 1995). Another approach was proposed and developed by Vanyan *et al.* (1995). The technique provides the best results when the submarine cable is perpendicular to the coastline. In this case the total electric field can be considered as sum of the 1D MT field and the TM anomalous field generated by electric charges at the coastline. The anomalous field increases

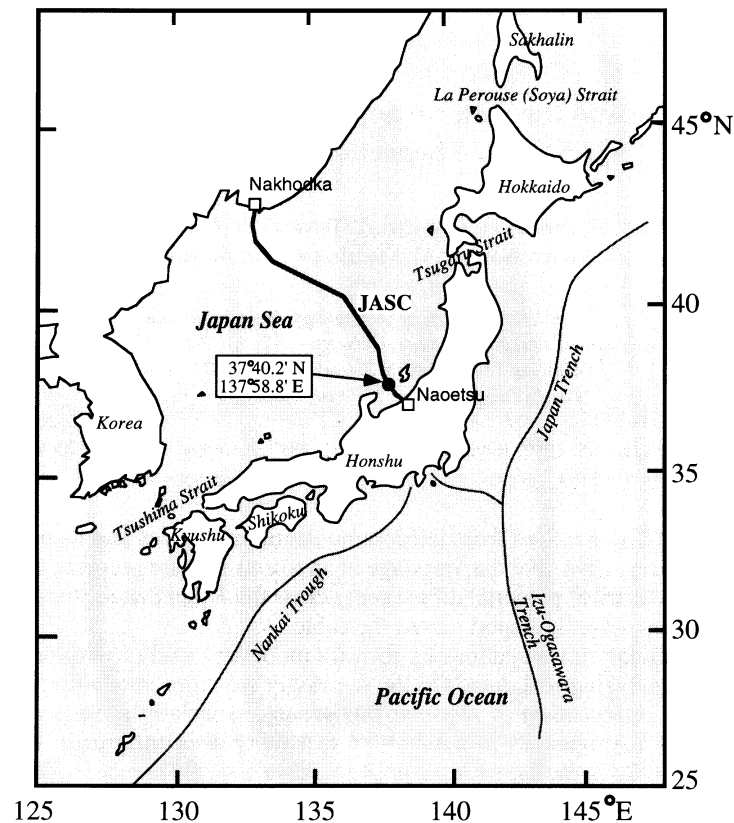


Fig. 1. Map of the Sea of Japan and the JASC position.

the total field on-shore and decreases it offshore (coast effect). The influence of the coast effect is reduced to some extent by electric current leakage to and from the asthenosphere (through the lithosphere). As a result the telluric field at the 'adjustment distance' from the coastline is more or less undistorted. It has been shown by many authors (e.g., Cox, 1980) that the typical scale can be estimated as a few multiples of the geometric mean of the water layer conductance and the lithosphere integrated resistivity. This feature of the adjustment distance suggests that the cable MT response shift will provide the information about the lithosphere integrated resistivity. For a first order approximation the latter is a resistivity-thickness product. On the other hand, TE mode MT response sensitivity to this parameter is poor.

The analysis of motionally induced electric field usually consists of removing MT-fields and signals of tidal frequencies (including solar-daily variations) and estimating the correlation coefficient with water transport across the cable. The correlation can be estimated with a help of water transport estimations by traditional oceanographic techniques or with a help of numerical modelling studies. The main problem is that cable voltage is proportional to the depth-averaged water velocity integrated along the cable and this is not exactly the water transport for the most of submarine cables (Larsen, 1992). Another problem that could be addressed by cable measurement is studying the synoptic and seasonal variability of the water velocity field (Chave *et al.*, 1997; Palshin *et al.*, 1996).

2. Observation

The location of the JASC is shown in Fig. 1. Geographical coordinates of the cable ends are $42^{\circ}48'N$ and $132^{\circ}49'E$ (Nakhodka) and $37^{\circ}10'N$ and $138^{\circ}14'E$ (Naoetsu). After its transfer to the scientific community, the Japanese end of the JASC had to be cut and removed from the coast to a point along the cable route where the water depth is 1,500 m (see Fig. 1). The cable end was cut at $37^{\circ}40.2'N$ and $137^{\circ}58.8'E$ on March 27, 1996 and was properly terminated by a standard grounding electrode made of titanium.

On January 29 and 30 of 1996, a measurement system was installed at the cable station Nakhodka and monitoring the natural voltage commenced. The system consists of a digital voltmeter with 6 and 1/2 digit resolution, a laptop computer, a GPS-controlled clock, and an 128 MB optical disk drive. Sampling is made every second, and the clock accuracy is designed to be about 1 msec using GPS control. Figure 2 schematically illustrates the configuration of the recording system at Nakhodka station. Before the off-shore termination, the Naoetsu end of the JASC was terminated either by station and beach grounds (from the beginning till February 14) or by beach ground (from February 14 till the off-shore termination). On the other hand, the Nakhodka end is always terminated by a ground made of titanium.

Figure 3(a) shows a record for seven months from February 1, 1996. One can see a gap in the voltage difference when the Japanese end of the JASC was cut and terminated by an electrode. Another gap can be seen at the beginning of

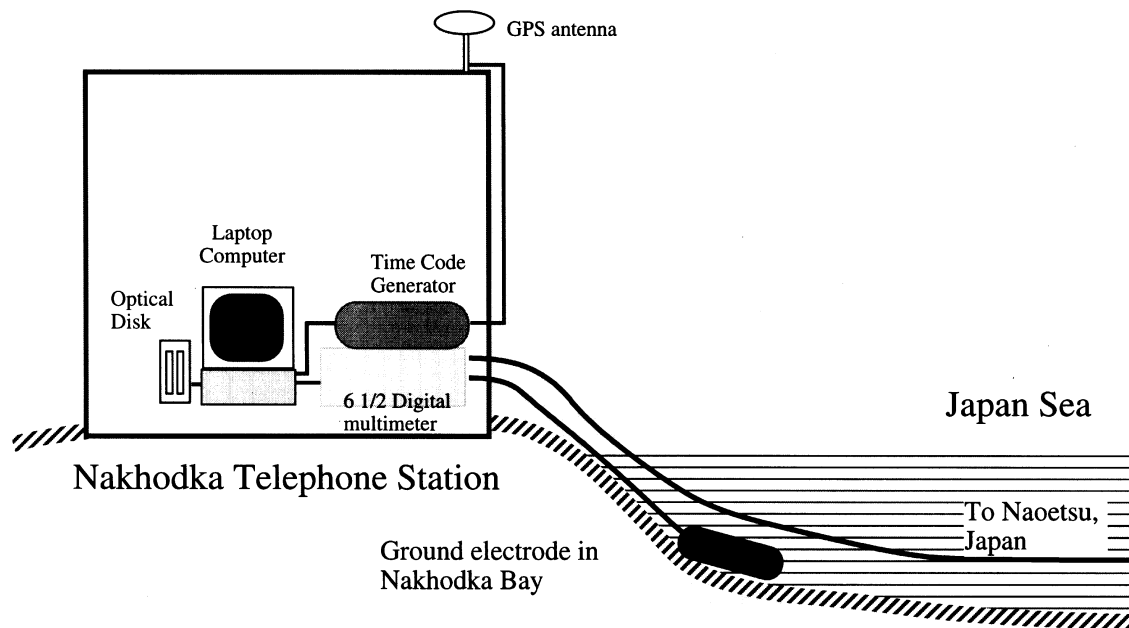


Fig. 2. Instrumentation for JASC voltage measurement installed at Nakhodka station.

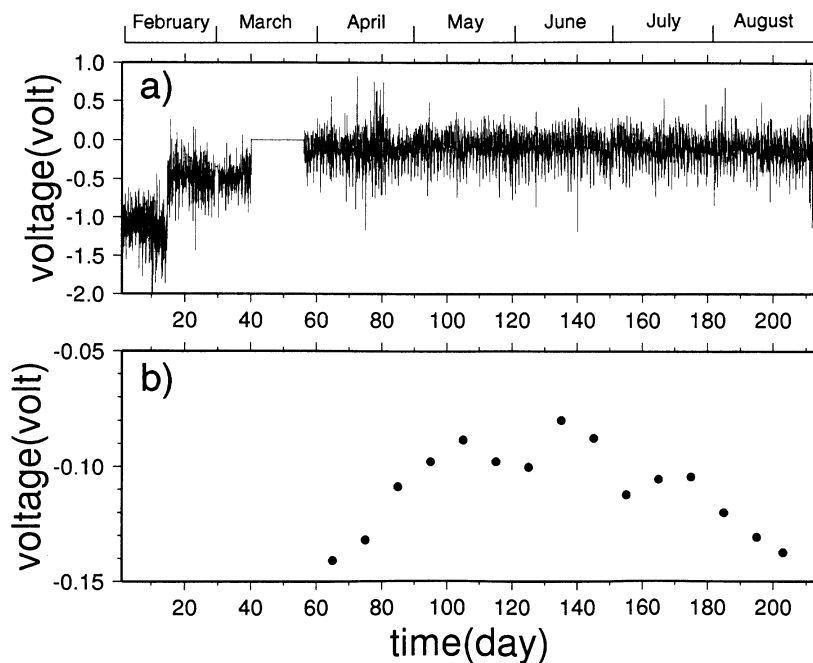


Fig. 3. Example of the voltage recording for seven months from February, 1996. Raw data (a) and 20 days averaged values (b) were plotted. Time axis indicates serial days from February 1, 1996. Cable grounding changed on day 17. The recording system was off line from the main cable from 40 to 57 during the cable removal cruise for safety.

the record in the middle of February, when the ground on the beach was isolated from the station ground at Naoetsu. After offshore termination, the potential difference looks to contain little DC component. This is probably because the same material is used for the electrodes at both ends. In order to see more clearly the gradual variation in the observed voltage, 20 days averages were obtained from the original record and

shown in Fig. 3(b). An increase and a decrease of 50–60 mV were found in the voltage for the first and last two months, respectively. Although the data length so far obtained is not enough to clarify its nature, this gradual variation may be reflecting an annual variation of the water transport in the Japan Sea. This time change will be compared with the numerical modelling result in the later section.

Table 1. 1D conductivity structure used in the forward modelling.

Layer	Thickness (km)	Resistivity (Ωm)
1	50	$5 \times 10^2, 2 \times 10^3, 5 \times 10^3, 1 \times 10^4$
2	150	10
3	100	30
4	300	10
5	∞	1

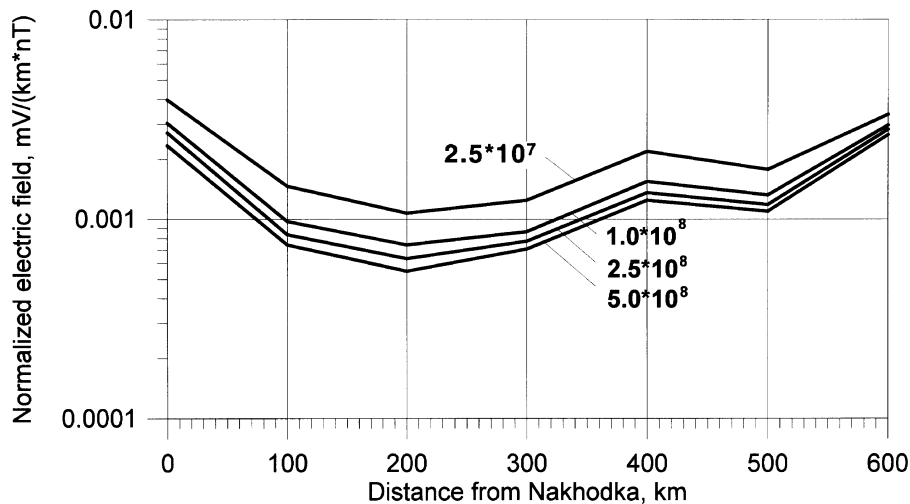


Fig. 4. Normalized MT electric field along the cable for various lithospheric resistance.

After the measurement had been thus started, it was found that there was clock error as much as 4 minutes during the seven months' recording. This error was found to be due to an instrumental trouble with the GPS time code generator. The trouble has already been solved, but the amount of data that has been recorded is still not sufficient for a detailed analysis. In this paper, therefore, no further time series analysis will be made, but only discussions on expected outcomes will be made based on forward modelling as shown in the following sections.

3. Forward Modelling of JASC Magnetotelluric Response

Numerical thin sheet modelling (Vasseur and Weidelt, 1977) was carried out to evaluate the sensitivity of the MT response derived from the cable data to the lithosphere resistivity. The laterally inhomogeneous water layer of the Sea of Japan and the sediment cover were considered as the thin-sheet with conductance $S(x, y)$. The off-shore conductance was calculated using the bathymetry data and an average conductivity value of 3 S/m. Cell width is 100 km. Conductance of the sea-floor sediments was added to the sea water conductance but the increase was not more than 7%. Average on-shore conductance was assumed to be constant (50 S) according to Semenov and Rodkin (1996), while conductivity distribution beneath the inhomogeneous thin sheet was assumed to be one dimensional with the lithosphere of 50

km thickness. Integrated resistivity of the lithosphere varied from 2.5×10^7 to $5 \times 10^8 \Omega\text{m}^2$ (see Table 1).

Simulated electric field component along the cable was normalized by the reference horizontal magnetic component (perpendicular to the JASC). Corresponding impedance values for the variation period $T = 10^6$ sec are shown in Fig. 4 for four values of the integrated resistivity. The general tendency is: the smaller the lithosphere resistivity, the greater is the electric field, or the less is the anomaly of the electric field associated with the Sea of Japan.

Real and imaginary parts of the normalized electric field were integrated along the cable and then divided by the cable length. The obtained impedance values were used for the "average" apparent resistivity calculation at the period range 1 hour–10 days. Corresponding apparent resistivity curves are shown in Fig. 5 for different values of the lithosphere resistivity. One can see the tendency in this figure: the smaller integrated resistivity, the greater apparent resistivity, although the shape of all curves are similar.

In order to examine the effect of the asthenosphere conductivity, numerical modelling was carried out for two values (0.05 and 0.1 S/m). In both cases the thickness of the asthenosphere was assumed to be of 100 km that corresponds to the conductance values 5000 and 10000 S. The former value was recently revealed for the Far East subduction zone (Semenov and Rodkin, 1996) while the latter one represents the largest value obtained in the Northern Pacific. However, we found

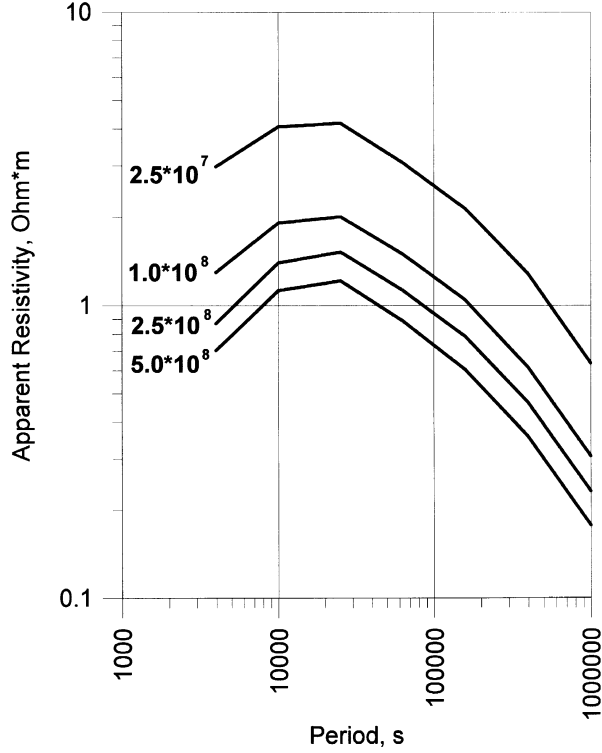


Fig. 5. JASC apparent resistivity for various lithospheric resistance.

that the results show little difference (only less than 2% of apparent resistivity) for periods greater than 10^5 sec.

4. Forward Modelling of Motionally Induced Electric Field

Two steps of numerical modelling technique were used for studying the spatial distribution of motionally induced electric field: In the first step the 3D water velocity field was simulated, and, in the second step the motionally induced electric field was calculated by using the velocity field obtained in the first step.

Water velocity field in the Sea of Japan was estimated with a stream function ψ and integrated vorticity ω . These two functions satisfy a system of two equations (Sarkisyan, 1977):

$$A\Delta\omega - \epsilon\omega = \frac{2\omega}{a} \frac{\partial\psi}{\partial\lambda} + \frac{f}{h} J(h, \psi - \psi_d) - \frac{\delta}{\rho} \text{rot}_z \vec{\tau} + \frac{\epsilon g}{\rho_0 f_0} \int_0^h z \Delta\rho' dz, \quad (1)$$

$$\Delta\psi = \omega, \quad (2)$$

where $\epsilon = \frac{f}{2\alpha h}$, $\alpha = \sqrt{\frac{f}{2k}}$, $\delta = \begin{cases} 1, & T_s > T_f \\ 0, & T_s \leq T_f \end{cases}$, T_s is the surface temperature, T_f is the freezing temperature of the sea water, $\psi_d = -\frac{g}{\rho_0 f_0} \int_0^h z \rho' dz$, λ is the geographic longitude; a is the Earth's radius; h is the sea depth; Δ is the horizontal Laplace operator; J is Jacobi operator; A , k are the coefficients of the horizontal and vertical turbulent exchange of the momentum; ρ is the water density ($\rho_0 = 1.027 \text{ g/cm}^3$), ρ' is

the deviation of the water density from the depth-averaged one (i.e. $\rho' = \rho - \rho_0$); $\vec{\tau}$ is the wind stress vector; g is acceleration of gravity; f is the Coriolis parameter, while f_0 denotes its latitudinal-mean value.

The equations (1) and (2) were solved using the no-flux and free-slip conditions on the boundaries: i.e., $\psi = \text{const}$, $\omega = 0$. Mesh intervals were 0.5 degrees for latitude and 0.25 degrees for longitude. Bottom topography, temperatures and salinity for winter and summer seasons at 9 levels (0, 50, 100, 150, 200, 300, 500, 1000, 2000 m) were taken from Levitus (1982) and interpolated on the numerical grid. Flow of the water into the Sea of Japan through the Tsushima Strait between Kyushu island and Korean peninsula was assumed to be of 1.8 Sv (winter) and 7.2 Sv (summer). Consequently the water flow out of the Sea of Japan was taken as 1.2 Sv and 0.6 Sv (winter) or 4.8 Sv and 2.4 Sv (summer) through the Tsugaru Strait between Honshu and Hokkaido islands and through the La Perouse (Soya) Strait between Hokkaido and Sakhalin islands, respectively.

Northward v and eastward u depth-averaged water velocity components can be obtained from the stream function ψ as:

$$v = \frac{1}{ah \cos\phi} \frac{\partial\psi}{\partial\lambda}, \quad u = -\frac{1}{ah} \frac{\partial\psi}{\partial\phi}, \quad (3)$$

where ϕ is the geographic latitude.

Calculated depth-averaged velocity components were used for simulation of the motionally induced electric field. The problem can be addressed by numerical thin-sheet modelling that is a good approximation for 3D modelling (Palshin *et al.*, 1996). The main features of this technique are:

- the frequency of changes in the water velocity is low, so the anomalous electric field \mathbf{E}_a can be treated as static and can be described by a scalar potential U : $\mathbf{E}_a = -\text{grad } U$;
- water depth, thickness of the sediment cover or of the upper resistive layers of the crust is thin compared with the horizontal dimensions, so that it is possible to consider a model consisting of two thin sheets. The first one is a conductive sheet with the conductance $S(x, y)$, i.e. the depth-integrated conductivity of sea water, bottom sediments and on-land conductive sediments. The second is a resistive sheet with depth-integrated resistivity $R(x, y)$ that simulates the resistive part of the Earth's crust. These sheets are underlain by a perfect conductor that simulates the conductive Earth's asthenosphere.

Continuity of electric current \mathbf{j} gives the following equation for the scalar potential U :

$$\text{div } \mathbf{j} = \text{div}[\sigma(\mathbf{V} \times B_z \hat{\mathbf{z}} - \text{grad } U)] = 0, \quad (4)$$

where σ is conductivity, \mathbf{V} is depth-averaged water velocity and B_z is vertical component of the Earth's magnetic field, and $\hat{\mathbf{z}}$ is a vertical unit vector.

2D divergence at the upper sheet can be obtained from (4):

$$\text{div}_2(\sigma \text{ grad } U) + \frac{\partial j_z}{\partial z} = \text{div}_2[\sigma(\mathbf{V} \times B_z \hat{\mathbf{z}})], \quad (5)$$

where j_z is the electric current directed downwards from the conductive thin sheet through the resistive one.

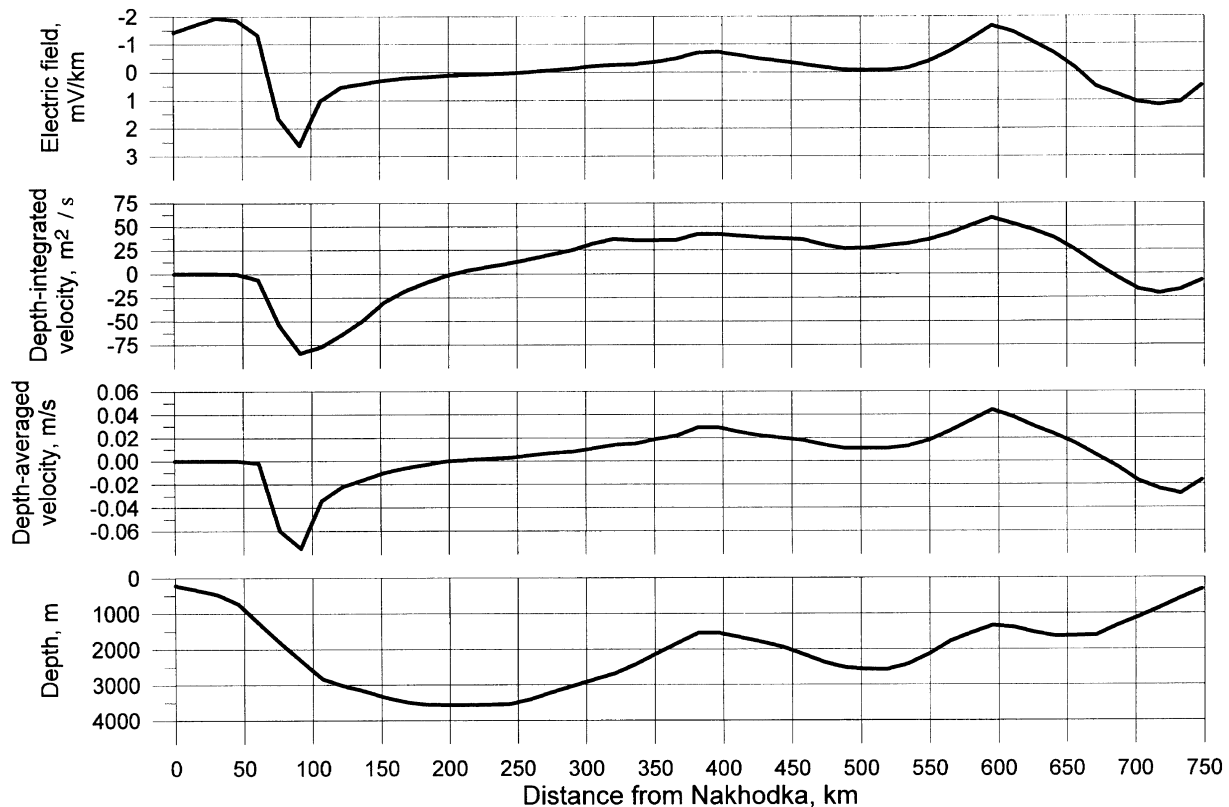


Fig. 6. Motional induced electric forward modelling results. Top curve is electric field. Second curve down is volume transport per unit width. Third curve down is depth averaged velocity. Bottom curve is bottom topography.

After integrating (5) along the vertical axis z we obtain:

$$\text{div}_2(S \text{ grad } U) + j_z = \text{div}_2[S_m(\mathbf{V} \times B_z \hat{\mathbf{z}})], \quad (6)$$

where S_m is the conductance of the moving water.

Taking into account that the scalar potential is zero at the bottom of the resistive sheet one can obtain $j_z = -U/R$. Finally the equation for scalar potential (4) could be presented as follows (Vanyan *et al.*, 1992):

$$\text{div}_2(S \text{ grad } U) - U/R = \text{div}_2[S_m(\mathbf{V} \times B_z \hat{\mathbf{z}})]. \quad (7)$$

The total electric field \mathbf{E} can be calculated as $\mathbf{E} = -\text{grad } U + \mathbf{V} \times B_z \hat{\mathbf{z}}$.

The finite element method employed by Vanyan and Yegorov (1992) and Yegorov and Palshin (1994) has been used to solve Eq. (7).

An example of modelling results is shown in Fig. 6 for summer conditions (water flow 7.2 Sv). The depth-averaged velocity component perpendicular to the cable is the result of the first step of the simulation procedure. The final result is the motionally induced electric field along the cable (upper panel).

5. Discussion

5.1 Study of the Sea of Japan lithosphere

Forward modelling results shown in Figs. 4 and 5 suggest the strong influence of the integrated resistivity of the lithosphere on the normalized electric field component along the cable. The electric field decrease caused by high conductance of the seawater layer reveals a clear dependence on the

integrated resistivity value. For instance, the electric field at the point 200 km east off Nakhodka decreases by a factor of two or so if the model integrated resistivity changes from 2.5×10^7 to $5 \times 10^8 \Omega\text{m}^2$.

The apparent resistivity curves were calculated using the electric field averaged along the cable and reference “undistorted” magnetic field component perpendicular to the cable direction. Calculated apparent resistivity curves have the same shape but their level depends strongly on the lithosphere integrated resistivity. This dependence is usually called the “static shift” and is considered as a distortion. In our technique the static shift is the main source of information about the conductivity structure of the lithosphere of the Sea of Japan.

The role of on-shore conductance should be discussed as well. The anomalous electric field is a result of the on-shore and offshore conductance contrast. The latter can be easily found using data available. Much less information could be obtained about the sediment cover conductance. So the question is: how strong will Fig. 5 change due to variations in on-shore conductance? Geological and conductivity data suggest a value about 50 S as a most probable sediment conductance estimate. An additional modelling was done for two values of the on-shore sediment cover conductance: 15 and 150 S. Electric field integrated along the cable decreases at 5% for the first value and increases at 10% for the second. Thus, the JASC voltage only slightly depends on the on-shore sediments conductance variation from 15 to 150 S.

The asthenosphere is the main path for the electric current

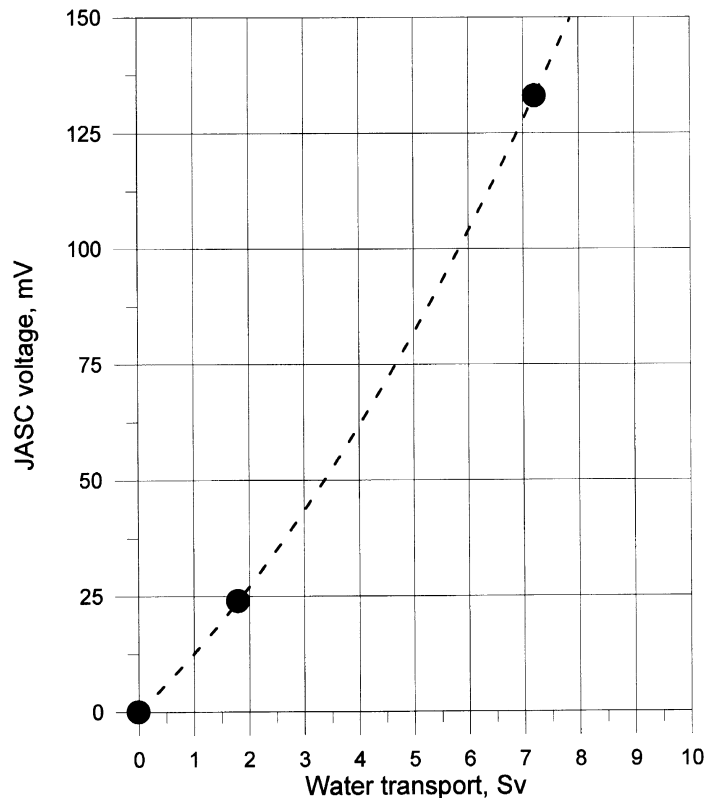


Fig. 7. Correlation of the total water transport across the cable and motionally induced cable voltage (forward modelling results).

flowing into the water layer and compensating the electric field decrease. Unfortunately the information about the conductance of the Sea of Japan asthenosphere is poor. An indirect estimation for the northern part of the Sea of Japan were made using MT study at Sakhalin Island (Semenov and Rodkin, 1996). The conductance of the asthenospheric partly molten zone was estimated to be of 5000 S. Utada *et al.* (1996) also suggested rather resistive asthenosphere beneath the Japan Sea based both on indirect information from magnetovariational and magnetotelluric array studies on land and on direct information from a seafloor magnetotelluric result. According to the geothermal data one can expect an increase of the asthenosphere conductance in the central part of the Sea of Japan. We believe 10000 S for the asthenosphere is an upper limit according to the sea-floor MT soundings made previously in the Pacific (Palshin, 1988). Modelling results using this value, however, showed that the change in voltage is less than 2% for periods greater than 10^5 sec. It was found the influence of the enhanced asthenosphere conductance is more significant for shorter periods. Therefore it is more reasonable to use the long-period part of the apparent resistivity curve for the lithospheric study.

5.2 Electric monitoring of water transport

An example of the velocity distribution along the JASC (Fig. 6) reveals some features of the cable voltage and water transport correlation. According to the forward modelling the sea current at the Russian shelf is directed southward while in the eastern part of the Sea of Japan it is directed northward. Thus, the total water transport across the cable is really the difference between the northward (warm) and

southward (cold) sea currents.

The electric field along the cable is similar to the depth-averaged velocity (Fig. 6). It means that electric field anomalies caused by the conductivity inhomogeneities do not significantly influence the cable voltage. After integrating the simulated electric field along the cable the correlation between cable voltage and water transport was estimated (Fig. 7). According to the estimation obtained, water transport of 5–6 Sv generates cable voltage of 70–80 mV. This estimation is consistent with the observation during five months (Fig. 3(b)), if the observed gradual variation corresponds to a part of annual variation.

6. Conclusions

Forward modelling results suggest that the TM (galvanic) mode of the MT field provides the major contribution to the telluric field along the cable. In spite of some influence of the on-land sediment conductance and asthenosphere conductivity, a significant dependence of the JASC voltage on the lithosphere integrated resistivity was revealed.

Two-step numerical modelling of the motionally induced electric field along the JASC reveals its similarity with the depth-averaged water velocity component perpendicular to the cable. The correlation coefficient obtained between the simulated JASC voltage and the water transport can be used for estimation of difference of the cold and warm water transports in the Sea of Japan.

Acknowledgments. JASC Project started due to courtesy of Koku-sai Denshin Denwa (KDD), ROSTELECOM and Great Northern

Telegraph Companies (GNTC). The authors are grateful to V. M. Nikiforov (Pacific Oceanographic Institute) for taking care of the instruments, and to N. Matsushima for help in preparing the figures. The manuscript was improved by helpful comments from reviewers (J. Larsen and A. White). Financial supports for this research from Russian Foundation for Basic Researches (Grant 96-05-66183), the Grant in Aid for Overseas Scientific Research by Ministry of Education, Science, Sports and Culture of Japan (Grant 06041025) and the Ocean Hemisphere Network Project (Grant 08-NP1101) are gratefully acknowledged.

References

- Chave, A. D. and D. S. Luther, Low-frequency, motionally induced electromagnetic fields in the ocean, 1. Theory, *J. Geophys. Res.*, **95**, 7185–7200, 1990.
- Chave, A. D., D. S. Luther, and J. H. Filloux, Observation of the boundary current system and heat transport at 26.5 N in the Subtropical North Atlantic Ocean, *J. Phys. Ocean.*, **27**, 1827–1848, 1997.
- Cox, C. S., Electromagnetic induction in the oceans and inferences on the constitution of the Earth, *Geophys. Surv.*, **4**, 137–156, 1980.
- Flosadottir, A. H., J. C. Larsen, and J. T. Smith, Motional induction in North Atlantic circulation models, *J. Geophys. Res.*, **102**, 10353–10372, 1997.
- Fujii, I., L. J. Lanzerotti, H. Utada, H. Kinoshita, J. Kasahara, L. V. Medford, and C. G. MacLennan, Geoelectric power spectra over oceanic distances, *Geophys. Res. Lett.*, **22**, 421–424, 1995.
- Kasahara, J., H. Utada, and H. Kinoshita, GeO-TOC project—Reuse of submarine cables for seismic and geoelectrical measurements, *J. Phys. Earth*, **43**, 619–628, 1995.
- Lanzerotti, L. J., A. D. Chave, C. H. Sayres, L. V. Medford, and C. G. MacLennan, Large scale electric field measurements on the Earth's surface: A review, *J. Geophys. Res.*, **98**, 23525–23534, 1993.
- Larsen, J. C., Transport and heat flux of the Florida Current at 27 N derived from cross-stream voltages and profiling data: Theory and observations, *Phil. Trans. R. Soc. Lond.*, **A 338**, 169–236, 1992.
- Levitus, S., Climatological atlas of the World ocean, *NOAA Profess. Pap.*, **13**, 1–173, 1982.
- Lizarralde, D., A. D. Chave, G. Hirth, and A. Schultz, Northeastern Pacific mantle conductivity profile from long-period magnetotelluric sounding using Hawaii-to-California submarine cable data, *J. Geophys. Res.*, **100**, 17837–17854, 1995.
- Palshin, N. A., Sea-floor deep magnetotelluric soundings in the northeastern Pacific, *Tikhookeanskaya Geologiya*, **6**, 95–99, 1988 (in Russian).
- Palshin, N. A., Oceanic electromagnetic studies. A review, *Surv. Geophys.*, **17**, 465–491, 1996.
- Palshin, N. A., L. L. Vanyan, and P. Kaikkonen, On-shore amplification of the electric field induced by a coastal sea current, *Phys. Earth Planet. Int.*, **94**, 269–273, 1996.
- Sanford, T. B., Motionally-induced electric and magnetic fields in the sea, *J. Geophys. Res.*, **76**, 3476–3492, 1971.
- Sarkisyan, A. S., The diagnostic calculations of large scale oceanic circulation, *The Sea*, **6**, 363–458, 1977.
- Semenov, V. Yu. and M. Rodkin, Conductivity structure of the upper mantle in an active subduction zone, *J. Geodynamics*, **21**, 395–364, 1996.
- Utada, H., Y. Hamano, and J. Segawa, Conductivity anomaly around the Japanese Islands, in *Geology and Geophysics of the Japan Sea*, pp. 103–149, Terra Sci. Publ., 1996.
- Vanyan, L. L. and I. V. Yegorov, Numerical modelling of the magnetotelluric field in the three-layered inhomogeneous media, *Fizika Zemli*, No. **7**, 121–125, 1992 (in Russian).
- Vanyan, L. L., T. A. Demidova, I. V. Yegorov, and R. P. Bulatov, Characteristics of electric field induced by Gulf Stream (Numerical simulation), *Phys. Solid Earth*, **28**, 339–342, 1992.
- Vanyan, L. L., N. A. Palshin, and I. A. Repin, Deep magnetotelluric sounding using submarine cable Australia - New-Zealand. 2. Interpretation, *Fizika Zemli*, No. **5**, 53–57, 1995.
- Vasseur, G. and P. Weidelt, Bimodal electromagnetic induction in non-uniform thin sheets with application to the Northern Pyrenean Anomaly, *Geophys. J. R. Astr. Soc.*, **51**, 669–690, 1977.
- Yegorov, I. V. and N. A. Palshin, Numerical modelling of the magnetotelluric fields in the inhomogeneous layered media, *Fizika Zemli*, No. **6**, 68–72, 1994 (in Russian).

L. L. Vanyan (e-mail: vanyan@geo.sio.rssi.ru), H. Utada (e-mail: utada@utada-sun.eri.u-tokyo.ac.jp), H. Shimizu, Y. Tanaka, N. A. Palshin, V. Stepanov, V. Kouznetsov, R. D. Medzhitov, and A. Nozdrina,